# General Disclaimer

## One or more of the Following Statements may affect this Document

- This document has been reproduced from the best copy furnished by the organizational source. It is being released in the interest of making available as much information as possible.

- This document may contain data, which exceeds the sheet parameters. It was furnished in this condition by the organizational source and is the best copy available.

- This document may contain tone-on-tone or color graphs, charts and/or pictures, which have been reproduced in black and white.

- This document is paginated as submitted by the original source.

- Portions of this document are not fully legible due to the historical nature of some of the material. However, it is the best reproduction available from the original submission.

Produced by the NASA Center for Aerospace Information (CASI)

N5G-7643

i

# SOLIDIFICATION MECHANISM OF HIGHLY UNDERCOOLED METAL ALLOYS

YUH SHIOHARA, MEN G. CHU, DAVID G. MACISAAC AND MERTON C. FLEMINGS
M.I.T., 77 Massachusetts Avenue, Cambridge, Massachusetts, USA

## ABSTRACT

This paper describes the results of experiments on metal droplet undercooling, and presents a preliminary analysis of the structures obtained. Work was conducted with Sn-25wt%Pb and Ni-34wt%Sn alloys. To achieve the required high degrees of undercooling, emulsification treatments were utilized following techniques described by Perepezko and co-workers.

Experiments show the fraction of supersaturated primary phase is found to be a function of the amount of undercooling, as is the fineness of the structures. The solidification behavior of the tin-lead droplets during recalescence was analyzed using three different hypotheses; 1) solid forming throughout recalescence is of the maximum thermodynamically stable composition, 2) partitionless solidification below the "$T_o$" temperature, and solid forming thereafter is of the maximum thermodynamically stable composition, and 3) partitionless solidification below the "$T_o$" temperature with solid forming thereafter that is of the maximum thermodynamically metastable composition that is possible.

## INTRODUCTION

Undercooling of liquid metal is a common phenomenon, but the amount of undercooling is usually restricted by the presence of heterogeneous nucleation catalysts. The homogeneous and heterogeneous nucleation theory was first applied to metallic systems by Turnbull and his co-workers [1]. The critical (maximum) undercoolings obtained were approximately equivalent to 0.18 $T_m$, where $T_m$ is the melting point of the metal in the absolute temperature scale.

Recently, the droplet technique has been modified and improved by Perepezko, Loper and co-workers [2,3]. Finely dispersed droplets of low melting temperature alloys, emulsified in an organic oil, have shown undercoolings in excess of 0.3 $T_m$ prior to nucleation.

In this work, high undercoolings were generated by the emulsification method and resulting microsegregation and the microstructure studied in Sn-25wt%Pb alloy. The technique was also extended for the first time to a high melting point nickel base alloy.

## EXPERIMENTAL PROCEDURE

The tin-lead alloy was prepared in a vacuum melter from high purity (99.9999%) metals. Droplet dispersions of the alloy were produced in a resistance furnace by emulsifying a mixture of liquid metal and organic carrier fluid (Polyphenyl-ether), contained a Pyrex crucible, with a high speed (3800 rpm) shearing device. The atmosphere in the furnace was purged with pure argon gas. Residual amounts of oxygen in the presence of isophthalic acid served as an oxidant to produce a thin oxide surface film, which prevents the

droplets from agglomerating. The temperature was kept at 25°C above the melting point during shearing, which continued for 40 minutes, producing fine droplets dispersed in the oil. The emulsified samples were transferred to sealed aluminum pans for analysis in a differential thermal analysis (DTA) or a differential scanning colorimeter (DSC) apparatus. The emulsified samples were removed from the aluminum pans and ultrasonically cleaned in preparation for observation of cross sectional microstructures by scanning electron microscope (SEM).

The emulsification method was modified for use with a nickel-tin alloy. Dispersions of the alloy in an oxide glass was carried out in an alumina crucible, under an inert atmosphere, with a mixing device also made of alumina. Undercoolings of large single droplets and droplet dispersions were measured by DTA.

## RESULTS

Tin-Lead Alloy. The emulsified droplets, observed with SEM, were distributed in the size range of 10-20 μm. A representative DTA result of about 15 mg of alloy and 20 mg of oil is presented in Fig. 1. The thermal heating curve of Sn-25wt%Pb (=16at%Pb) alloy shows two endothermic peaks due to melting. The first peak indicates the melting of eutectic regions. The second peak corresponds to the melting of primary tin rich phase. During cooling, one sharp exothermic peak due to solidification was observed. The amount of undercooling of most droplets is defined by the onset of this sharp peak. The shaded area in the figure is related to the latent heat of fusion for an alloy.



Fig. 1. Representative DTA results of a Sn-25wt%Pb droplet emulsion.

Figure 2 shows the cross sectional microstructure of a typical droplet which was solidified at a sample cooling rate of 10°C/min. Undercooling was measured as 80°C. The microstructure observed consists of a tin rich region surrounding a smaller lead rich region. The volume fraction of the lead rich region was estimated at 7%. This fraction was found to decrease with increasing cooling rate.

Following the same heating and cooling treatment, a specimen was reheated to 1°C higher than the eutectic temperature, held for 10 minutes (primary phase remained as a solid), and then cooled at the 10°C/min cooling rate. The undercooling for the eutectic solidification was measured as 6-9°C by DTA. The microstructure of this sample is shown in Fig. 3. Note that the lead rich eutectic now surrounds the primary tin rich phase.

Nickel-Tin Alloy. The sizes of the dispersed droplets produced by Ni-34wt%Sn ranged from 5-3000 μm. Fig. 4 shows SEM micrographs of several of these droplets. The predominant phase in all these structures was analyzed as the hypo-eutectic (tin rich) phase. Figs. 4a and 4b show structures of coarse droplets of the same size (2 mm), nucleated at different temperatures. The finest structure corresponds to the highest undercooling. The droplets in Figs. 4c and 4d are much smaller in size (700 μm and 60 μm diameter respectively); both are from a single dispersed droplet DTA run in which the undercooling was measured as a single peak. Note the structure is finer in the smaller of these droplets and both these structures are much finer than those in Figs. 4a and 4b.
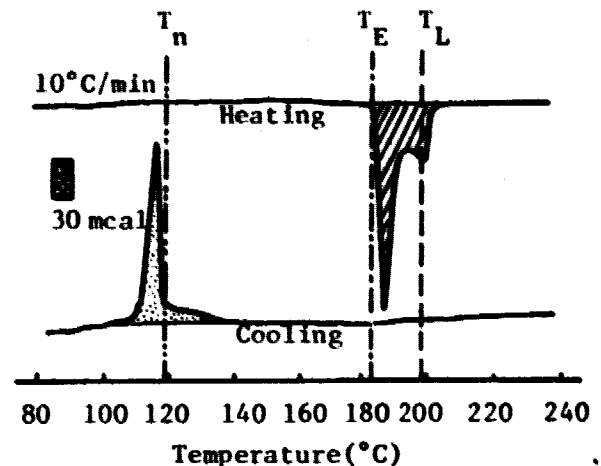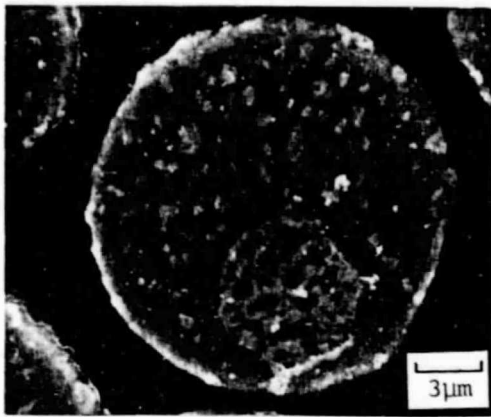
Fig. 2. Cross sectional microstruc-
ture of a Sn-25wt%Pb droplet after
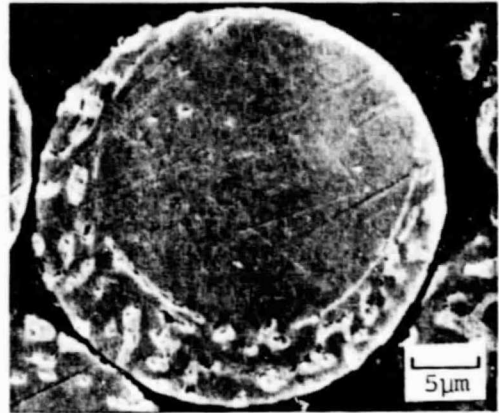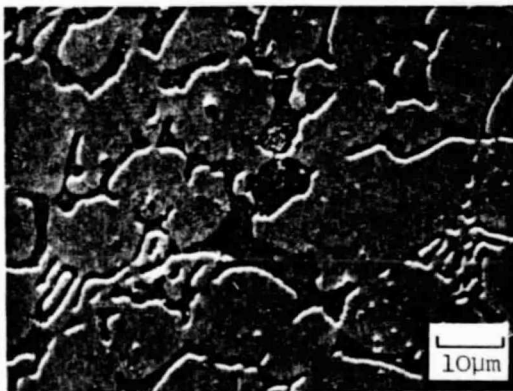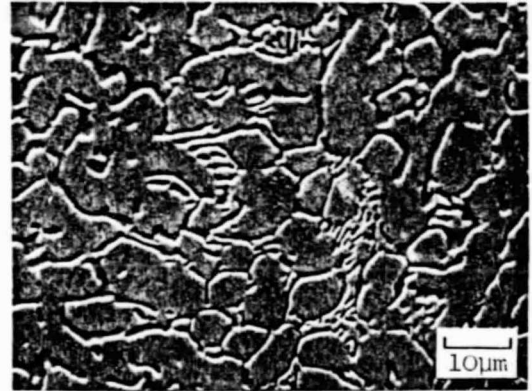solidification at a cooling rate of
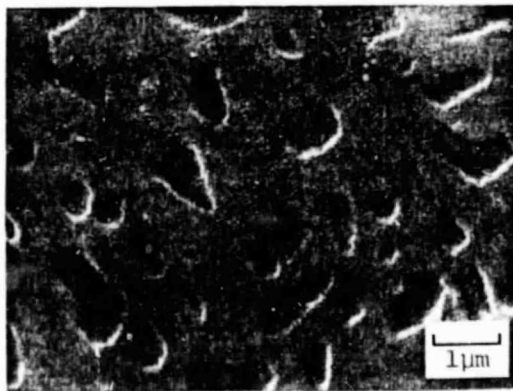10°C/min and with 80°C of undercooling.

Fig. 3. Cross sectional microstruc-
ture of a Sn-25wt%Pb droplet in which
the eutectic region was remelted at
1°C higher than the eutectic tempera-
ture and then cooled at 10°C/min.

(a)

(b)

(c)

(d)

Fig. 4. Cross sectional microstructure of Ni-34wt%Sn droplets.
(a) Droplet diameter (D) = 2 mm, undercooling ($\Delta T$) = 88°C.
(b) D = 2 mm, $\Delta T$ = 177°C.
(c) D = 0.7 mm, $\Delta T$ = 219°C.
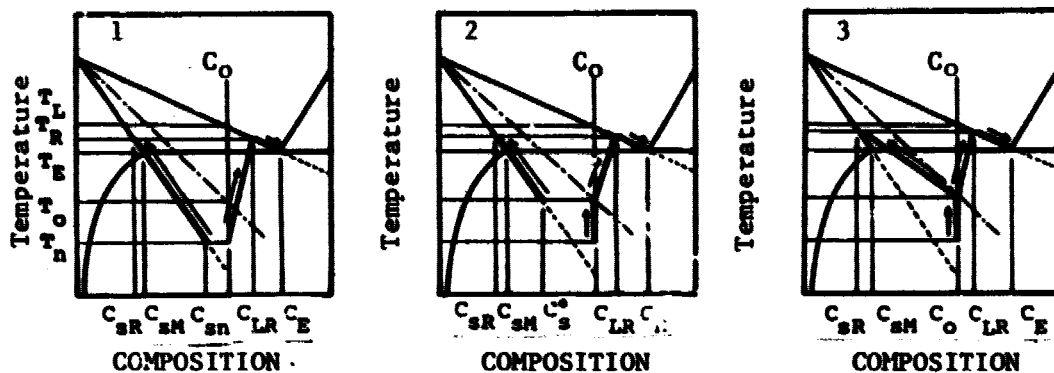(d) D = 0.06 mm, $\Delta T$ = 219°C.

Fig. 5. Schematic illustration of the solidification paths for three solidification models.

## DISCUSSION

In order to interpret the structures and segregation obtained in undercooled specimens we have carried out detailed calculations of solidification behavior using the three models to be discussed below. Complete calculations and extensions of these models are described in a separate paper [4]. Assumptions common to all three models are 1) no solid diffusion, 2) no remelting during recalescence, 3) adiabatic conditions during recalescence and 4) negligible thermal gradients in the droplets during solute redistribution, and after recalescence, solidification proceeds according to the Scheil equation.

In Case 1, solid forming throughout solidification is assumed to be of the maximum thermodynamically stable composition. Hence initial solid forms of compositions along the solidus from $C_{sn}$ at the nucleation temperature to $C_{sR}$ at the maximum recalescence temperature. If diffusion in the liquid is essentially complete, liquid composition follows the line shown in Fig. 5 for Co to $C_{LR}$ during recalescence. After recalescence, solidification occurs by the Scheil equation with the primary solid composition reaching a maximum of $C_{sM}$ and the liquid reaching a maximum of eutectic composition, $C_E$ [5]. Fig. 6, curve 1, shows the solute redistribution expected across a cell or dendrite of Sn-16at%Pb alloy undercooled 80°C and solidified according to these assumptions.



Fig. 6. Calculated solute redistribution profiles for three solidification models, Sn-16at%Pb.

In Case 2, solidification is assumed partitionless between $T_N$ and $T_O$ so solid composition is $C_O$. The "$T_O$" temperature is calculated from the equal molar free energies of the liquid and the solid using the regular solution approximation. The dependence of the temperature on the molar free energy is
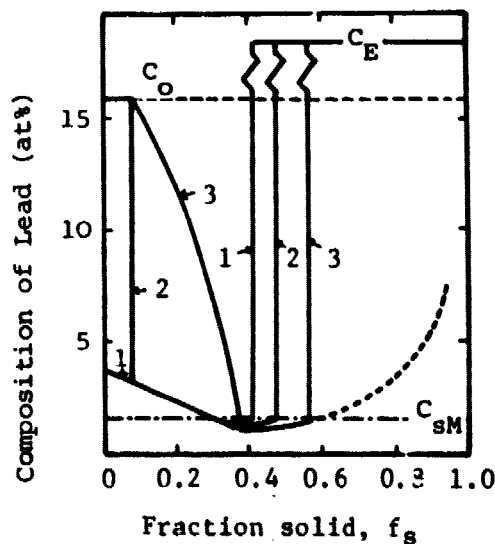
calculated from the Gibbs-Helmholtz relationship. Above $T_0$, solidification is as in Case 1.

In Case 3, solidification below $T_0$ is partitionless as in Case 2. Above $T_0$, the solid composition at the interface is the maximum thermodynamically possible solubility. This composition, $C_s$, is calculated from the intersection of the molar free energy curve for the solid and tangent line to the molar free energy curve for the liquid at the composition $C_L$, as described by Cahn [6].

On the basis of microstructures obtained to date, it is not possible to distinguish between the three mechanisms discussed above. Composition calculations based on lineal analysis of volumes of the two phase present in the photomicrograph of Fig. 2 indicate the composition of the large tin rich region is just below $C_0$ (about 22wt%Pb) and the small lead rich region is about 65wt%Pb. If Case 1 applies, liquid must have been entrapped during growth of the large tin rich region. If the small region represents solidification of eutectic liquid after its recalescence, its amount (estimated volume fraction .07) is much lower than that of any of the three cases considered, in which predicted fraction eutectic varied from about 0.45 to 0.6, and its composition is much higher than would be expected. It is clear that other factors must be considered in predicting solute redistribution in these samples, including perhaps heat flow during and after recalescence, remelting and ripening, eutectic undercooling, and metal shrinkage or expansion during solidification.

Fig. 3, obtained by holding 10 minutes at 1°C above the eutectic temperature and then cooling shows two significant effects. One of these is the dramatic change in shape of the primary solid by ripening and the other is the coarse lamellar type eutectic structure typical of eutectic solidification at low undercoolings [7]. Both those effects may need to be considered in a full analysis of the original undercooled structure.

The fineness of the Ni-Sn structure, as well as the "eutectic" structure of the Sn-Pb alloy is indicative of extremely rapid solidification rates. The structure of the large Ni-Sn droplet, solidified at high undercooling, is only about 5µm while that in the 60µm diameter particle is less than about 1µm even though the cooling rate of the specimens was only about 50°C/min. Local heat extraction from the individual droplets into the surrounding fluid must be an important factor influencing these structures.

ACKNOWLEDGEMENT

REFERENCES

1. D. Turnbull and R.E. Cech, J. Applied Physics, 21, 805 (1950).

2. J.H. Perepezko, D.H. Rasmussen, I.E. Anderson and C.R. Loper, Jr., Proceedings of International Conference on Solidification, The Metal Society, 169 (1977).

3. J.H. Perepezko and I.E. Anderson, TMS-AIME Symposium on Synthesis and Properties of Metastable Phases, T.J. Rowland and E.S. Machlin eds. In press.

4. M.C. Flemings, Y. Shiohara, M.G. Chu and D.G. MacIsaac, to be published.

5. T.Z. Kattamis, Zeitschrift fur Metallkunde, 61, 856 (1970).

6. J.C. Baker and J.W. Cahn, Solidification (American Society for Metals, Metals Park, Ohio, 1971) p. 23.

7. T.Z. Kattamis and M.C. Flemings, Trans. AIME, 236, 1523 (1966).